Improving the spectral resolution of fMRI signals through the temporal de-correlation approach

Anonymous Author(s)
Affiliation
Address
email

Abstract

The inherent infra-slow, narrowband signal thwarts the fMRI modality in considering as an optimal neuroimaging modality to its alternatives, e.g., EEG and MEG, in investigating the spectral character of cortical activities. To enhance the spectral resolution of fMRI signal, we put forward a novel linear transformation approach to encourage both the multivariate fMRI time series and their derived temporal derivatives to be temporal de-correlated with each other. Thorough empirical validations of our temporal de-correlation approach on multiple independent fMRI datasets are presented, along with the attached empirical comparison of several alternative methods. Throughout all employed fMRI datasets, we observe a general increment on spectral resolution of temporal de-correlated fMRI signals in terms of wider frequency bandwidth, and more distinctive spectral characters to the original signals.

1 Introduction

In studying the rhythmic brain oscillations, among common neuroimaging modalities, e.g., electroencephalogram (EEG), magnetoencephalography (MEG), and functional magnetic resonance imaging (fMRI), the fMRI modality is long been regarded as the least suitable modality in spectral analysis. As illustrated in Figure 1(a), in comparison with the broad spectral resolutions of EEG and MEG modalities, the spectral resolution of fMRI modality is confined to $0.01 - 0.25$ Hz [1] [2], occupied the mere slow-4 and slow-3 classes among a spectrum of frequency classes [3]. Aside from the confronted narrowband issue of fMRI modality, relying on our defined spectral character, i.e., the intrinsic frequency of a signal (see attached Appendix A), the lowered spectral resolution of fMRI signals is further exacerbated by the presented spectral homogeneity. As reflected in Figure 1(b)(c), irrespective of the harnessed parcellation atlases, and employed fMRI datasets, the attained spectral characters of fMRI signals are distributed in a tightly-clustered, indiscriminating manner.

To improve the spectral resolution of fMRI signals in attaining discriminating spectral characters, we propose a linear transformation approach that aims at reconstructing a temporal de-correlated version of the original fMRI signals to encourage both signals and the derived temporal derivatives are temporally independent. The remaining article is organised as follows. After a detailed description of our proposed method in §2, the following section §3 presents the empirical validation of our approach on various fMRI datasets in the face of alternative methods. The final section §4 concludes the article, and highlights two potential applications in future neuroscientific research.

Submitted to 35th Conference on Neural Information Processing Systems (NeurIPS 2021). Do not distribute.

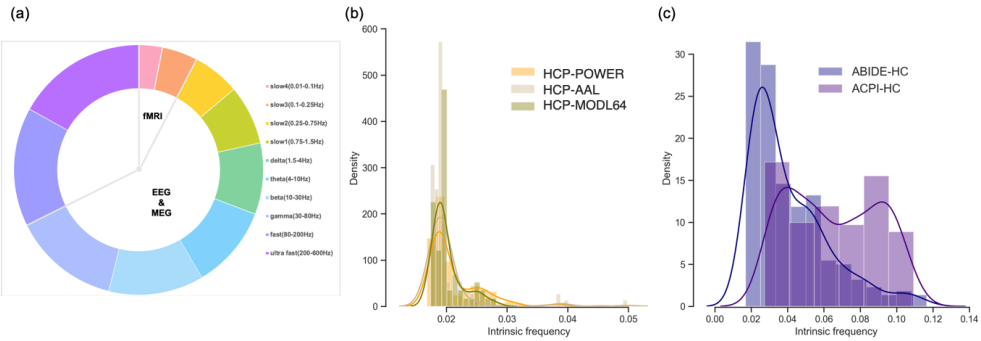

Figure 1: **Spectral limits of fMRI signals.** (a) The infra-slow, narrowband fMRI signals. In comparison with the broadband EEG and MEG signals, the fMRI signals can merely occupy the slow-4 and slow-3 frequency classes [3]. (b) Spectral homogeneity of fMRI signals with respect to different parcellation schemes. Taking the example of HCP data [4], irrespective of the harnessed parcellation atlases, e.g., the Power [5], AAL [6], MODL64 [7] parcellation atlases, the presented spectral characters of fMRI signals are distributed in forms of tight-clustered, unimodal distributions. (c) Spectral homogeneity of fMRI signals across multiple fMRI datasets. The previous presented unimodal distribution of spectral characters is universally seen in fMRI datasets other than HCP, e.g., the ABIDE-HC [8] and ACPI-HC datasets. The details on deriving the sub-figures (b) and (c) are delineated in attached Appendix B.

2 Temporal de-correlation approach

Given I dimensional normalised multivariate time series X, i.e., $X(t) = [x_1(t), x_2(t), ..., x_i(t)]^T$, and, $\langle x_i(t)\rangle_t = 0, \langle x_i(t)^2\rangle_t = 1$, our temporal de-correlation approach entails the search for a series of vectorial embedding function $\mathcal{G}$, to project the original time series X onto a novel J dimensional functional space $\mathcal{F}$, i.e., $\mathcal{G}(X) = [g_1(x), g_2(x), ..., g_j(x)]^T$. Hence, as illustrated in the presented scheme (Figure 5), the original time series is firstly embedded as $y_j(t) := g_j(x(t))$ on a new functional space $\mathcal{F}$.

Armed with J dimensional embedded signals, our task is to find the optimal embedding function that enforces both embedded signals $y_j(t)$, and their temporal derivatives, i.e., $\Delta(y(t)) := \langle \dot{y}\rangle_t$, to be temporal de-correlated with each other. Thus, the temporal de-correlation approach can be regarded as an optimisation problem, which is stated as:

$$\begin{aligned} &\text{minimize} \;\; \langle \dot{y}_j(t)\dot{y}_{j'}(t)\rangle_t \\ &\text{subject to} \;\; \langle y_j(t)y_{j'}(t)\rangle_t = 0; \;\; \forall y_{j'}(t) \neq y_j(t), \end{aligned} \tag{1}$$

where $\langle\cdot\rangle_t$ represents the temporal averaging of t length time series.

Assuming $\mathcal{G}()$ as a series of linear embedding functions, and the one-to-one mapping between the original and embedded functional space, i.e., $I = J$, to search for the optimal linear embedding function is equivalent of finding the optimal W matrix, where w_j indicates its j-th row vector. The foregoing optimisation problem can be further derived as:

$$\begin{aligned} &\underset{w}{\text{minimize}} \;\; w_j w_{j'}^T \Sigma_{\dot{x_i}\dot{x_{i'}}} \\ &\text{subject to} \;\; w_j w_{j'}^T \Sigma_{x_i x_{i'}} = 0; \;\; \forall x_{i'}(t) \neq x_i(t), \end{aligned} \tag{2}$$

where $\Sigma_{x_i x_{i'}}$, and $\Sigma_{\dot{x_i}\dot{x_{i'}}}$ denote the covariance matrix of the original input X, and the matrix of the second moments of the temporal derivative of X. Since the assumed one-to-one mapping between original and embedding space, two above-mentioned matrices are symmetric, i.e., $\Sigma_{x_i x_{i'}} \in \Re^{I\times I}$, and $\Sigma_{\dot{x_i}\dot{x_{i'}}} \in \Re^{I\times I}$. With two symmetric matrices, the Lagrangian of foregoing optimisation renders us $\mathcal{L} = w_j w_{j'}^T \Sigma_{\dot{x_i}\dot{x_{i'}}} - \lambda(w_j w_{j'}^T \Sigma_{x_i x_{i'}})$, in which $\lambda \in \Re$ acts as the Lagrange multiplier [9]. As a result, the search for the optimal embedding function to yield our temporal de-correlation objective can be seen as solving the following generalised eigenvalue problem [10]:

$$\Phi\Sigma_{\dot{x_i}\dot{x_{i'}}} = \Lambda\Phi\Sigma_{x_i x_{i'}}; \; \forall x_i \neq x_{i'}, \tag{3}$$

where the columns of $\Phi := [\phi_1, ..., \phi_i]$ are the orthogonal eigenvectors, in which diagonal elements of $\Lambda := \mathbf{diag}([\lambda_1, ..., \lambda_i])^T$ are the eigenvectors.

Thence, for any multivariate time series X, we can always find a series of linear transformation $\mathcal{G}()$ in the embedded functional space $\mathcal{F}$ to allow the transformed signals to be temporal de-correlated in terms of their linear correlation and 1st-order temporal derivatives. We refer these transformed (reconstructed) signals as **temporal de-correlated signals**

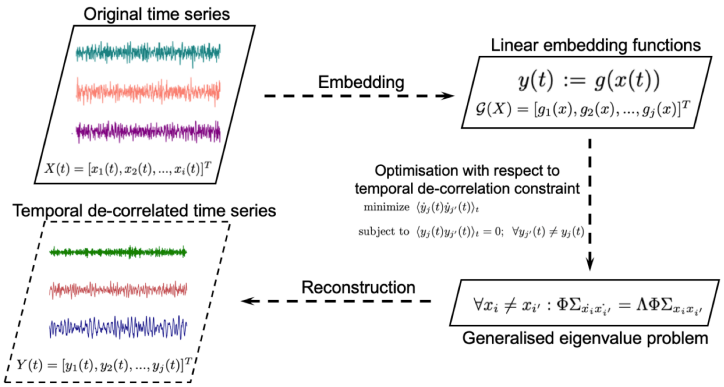

Figure 2: **Scheme of the temporal de-correlation approach** The implementation of the temporal de-correlation approach can be divided into three consecutive steps. Firstly, the original time series are embedded with linear embedding functions with ensured one-to-one mapping. The followed optimisation step degrades the search for the optimal embedding functions as solving an optimisation problem with the temporal de-correlate constraint. This can be further realised as solving a generalised eigenvalue problem. Armed with the derived optimal embedding functions, these output time series are our targeted **temporal de-correlated signals**.

3 Empirical experiments on real fMRI datasets

Seeking to validate our approach, we chiefly implement our temporal de-correlation approach on fMRI signals from the Human Connectome Project (HCP) [4]. For the validation purpose, we also incorporate the curated fMRI signals of healthy subjects from ABIDE (ABIDE-HC) and ACPI (ABIDE-HC) databases as two validation datasets. The details of three datasets are rendered in attached Appendix C. These subject-level fMRI signals are further averaged to produce the group-level fMRI signals for our analysis.

Focusing on the estimated spectrum of original and temporal de-correlated HCP fMRI signals, as demonstrated in following Figure 3, a clear spectrum differentiation is observed only in temporal de-correlated signals, whereas the spectra of original fMRI signals are rendered in a highly similar manner. The observed spectrum differentiation, in which the transformed signals are encouraged to be spectral distinctive from each other, suggests the increment on the spectral resolution of temporal de-correlated fMRI signals.

More evidently, with respect to the distributions of assessed spectral characters, i.e., the intrinsic frequencies of signals, two types of signals render us two drastically different distributions of spectral characters. As shown in Figure 4(a), on HCP dataset, the spectral characters of original signals are presented in the form of a tightly-clustered, unimodal inclined distribution, whereas the spectral characters of temporal de-correlated signals are distributed in the form of a bimodal distribution (Dip test statistic [11]: 0.0296 [1]). Notably, as shown in Figure 4(b), the observed divergent distributions of spectral characters between two types of signals are also reproducible on two validation datasets. In addition, in the face of other transformation approaches that enforce the similar temporal de-correlation constraint, it is of rising interest to empirical compare our approach with existing methods, e.g., the functional principal component analysis (FPCA) [12], the coroICA [13] the second-order ICA (SOBI) [14]. To interested readers, we attach the conducted empirical comparison among mentioned models in Appendix D.

[1] A Dip test value less than 0.05 indicates significant bimodality [11].

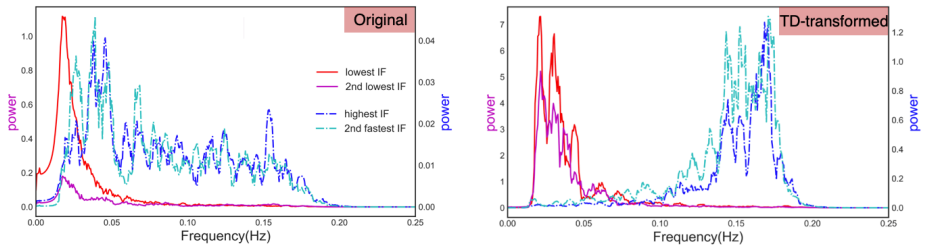

Figure 3: **Estimated spectrum of the original and temporal de-correlated fMRI signals.** Taking the example of HCP fMRI signals, the estimated spectrum from the original and temporal de-correlated fMRI signals are presented in the left and right panels, respectively. To ease the demonstration, the four most representative spectra, e.g., the spectra that are characterised as lowest, 2nd lowest, highest, and 2nd high intrinsic frequencies, are presented here. Abbreviation index: IF: intrinsic frequency; TD-transformed: temporal de-correlation transformed.

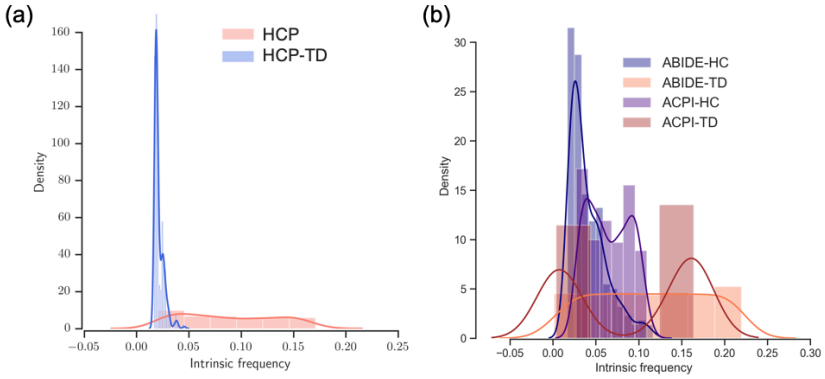

Figure 4: **Distributions of spectral character from the original and temporal de-correlated signals.** (a) Distributions of assessed spectral characters from the original and temporal de-correlated HCP fMRI signals. (b) Distributions of assessed spectral characters from the original and temporal de-correlated ABIDE and ACPI fMRI signals. Abbreviation index: HCP\ABIDE\ACPI-TD: the temporal de-correlated signals that are transformed from HCP\ABIDE\ACPI datasets.

In addition to the observed spectrum differentiation and bimodal distributed spectral characters, the improvement on spectral resolution of temporal de-correlated fMRI signals is also indicated in enlarged spectral dissimilarity, which is assessed through the computed dynamic time warping distance matrices on estimated spectrum of original and transformed signals (see attached Appendix E).

4 Conclusion

In summary, the major obstacle in spectral characterisation of fMRI signals lies on their inferior spectral resolution, thwarting the harnessing of fMRI modality in spectral analysis of recorded cortical activities. To enhance the spectral resolution of fMRI signals, we put forward a linear transformation approach, aiming at producing temporal de-correlated fMRI signals. Validated on three empirical datasets, a robust, and reliable increment on spectral resolution suggests the potential of our approach in future research.

With improved spectral resolution, these temporal de-correlated fMRI signals are expected to be implicated in a wide range of neuroscientific discoveries, including the production of a fine-grained spectral characterisation of cortical activities on the basis of fMRI modality, and an in-depth probe on the spectral characterisation of diverse neuropsychiatric disorders.

References

[1] Ali M Golestani, Catie Chang, Jonathan B Kwinta, Yasha B Khatamian, and J Jean Chen. Mapping the end-tidal co2 response function in the resting-state bold fmri signal: Spatial specificity, test–retest reliability and effect of fmri sampling rate. *NeuroImage*, 104:266–277, 2015.

[2] Nicole H. Yuen, Nathaniel Osachoff, and J. Jean Chen. Intrinsic frequencies of the resting-state fMRI signal: The frequency dependence of functional connectivity and the effect of mode mixing. *Frontiers in Neuroscience*, 13, 2019.

[3] György Buzsáki and Andreas Draguhn. Neuronal oscillations in cortical networks. *Science*, 304(5679):1926–1929, 2004.

[4] David C Van Essen, Stephen M Smith, Deanna M Barch, Timothy EJ Behrens, Essa Yacoub, Kamil Ugurbil, Wu-Minn HCP Consortium, et al. The wu-minn human connectome project: an overview. *NeuroImage*, 80:62–79, 2013.

[5] Jonathan D Power, Alexander L Cohen, Steven M Nelson, Gagan S Wig, Kelly Anne Barnes, Jessica A Church, Alecia C Vogel, Timothy O Laumann, Fran M Miezin, Bradley L Schlaggar, et al. Functional network organization of the human brain. *Neuron*, 72(4):665–678, 2011.

[6] Nathalie Tzourio-Mazoyer, Brigitte Landeau, Dimitri Papathanassiou, Fabrice Crivello, Olivier Etard, Nicolas Delcroix, Bernard Mazoyer, and Marc Joliot. Automated anatomical labeling of activations in spm using a macroscopic anatomical parcellation of the mni mri single-subject brain. *NeuroImage*, 15(1):273–289, 2002.

[7] Arthur Mensch, Julien Mairal, Bertrand Thirion, and Gaël Varoquaux. Dictionary learning for massive matrix factorization. In *International Conference on Machine Learning*, pages 1737–1746. PMLR, 2016.

[8] Adriana Di Martino, Chao-Gan Yan, Qingyang Li, Erin Denio, Francisco X Castellanos, Kaat Alaerts, Jeffrey S Anderson, Michal Assaf, Susan Y Bookheimer, Mirella Dapretto, et al. The autism brain imaging data exchange: towards a large-scale evaluation of the intrinsic brain architecture in autism. *Molecular psychiatry*, 19(6):659–667, 2014.

[9] Stephen Boyd, Stephen P Boyd, and Lieven Vandenberghe. *Convex optimization*. Cambridge university press, 2004.

[10] Beresford N Parlett. *The symmetric eigenvalue problem*. SIAM, 1998.

[11] John A Hartigan, Pamela M Hartigan, et al. The dip test of unimodality. *Annals of statistics*, 13(1):70–84, 1985.

[12] Roberto Viviani, Georg Grön, and Manfred Spitzer. Functional principal component analysis of fmri data. *Human brain mapping*, 24(2):109–129, 2005.

[13] Niklas Pfister, Sebastian Weichwald, Peter Bühlmann, and Bernhard Schölkopf. Robustifying independent component analysis by adjusting for group-wise stationary noise. *Journal of Machine Learning Research*, 20(147):1–50, 2019.

[14] Adel Belouchrani, Karim Abed-Meraim, J-F Cardoso, and Eric Moulines. A blind source separation technique using second-order statistics. *IEEE Transactions on signal processing*, 45(2):434–444, 1997.

[15] Behtash Babadi and Emery N Brown. A review of multitaper spectral analysis. *IEEE Transactions on Biomedical Engineering*, 61(5):1555–1564, 2014.

A Spectral character: the intrinsic frequency

To define the spectral character of a given time series, we firstly estimate the power spectrum densities (PSD) of a time series. Having I dimensional time series $x(t)$, the PSD of the i-th $x(t)$ via Fourier transform can be written as:

$$x_i(f) := \delta_t x_i(t) e^{-i2\pi t\delta(t)},$$

where the $\delta(t)$ denotes the sampling interval, and the $e^{-i2\pi t\delta(t)}$ is a periodic (sinusoid) function. The power of the i-th time series $x_i(t)$ in the frequency band $f \pm \frac{1}{2}\delta_t f$ is approximated as $P_i := \frac{1}{\delta(t)}|x_i(f)|^2\delta f$.

To reduce the PSD estimation bias, we further utilise the tapering technique [15] to construct a set of K different orthogonal data tapers h_t, i.e., $h_t^1, h_t^2, ..., h_t^k$. The multi taper spectral estimate of the i-th time series $x_i^{mt}(f)$ is then given by:

$$x_i^{mt}(f) := \frac{1}{K}\sum_{i=1}^{K} \hat{x}_i(f)$$

where

$$\hat{x}_i(f) := \delta_t |h_t^i x_i(t) e^{-i2\pi t\delta(t)}|^2,$$

such that the power of $x_i(f)$ in its frequency band $f \pm \frac{1}{2}\delta f$ can be multi taper estimated as $P_i^{mt} := \frac{1}{T}|h_t x_i(t)|^2 \delta_t f$.

To maximally reserve the spectral information of a time series, spectral filters were not applied in this spectral estimate. On the basis of the spectral estimate of a time series, its quantification on peak power frequency f_{peak}, which carries the maximum energy (power) among all frequencies along the spectrum, is defined as our spectral character, referring as the **intrinsic frequency** of a time series.

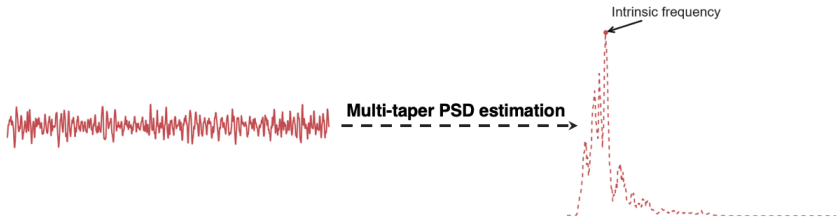

Figure 5: **Scheme of attaining the intrinsic frequency of a time series.** To assess the intrinsic frequency of a given time series, its spectrum is estimated via introduced multi-taper PSD estimation method. On the estimated spectrum, the peak power frequency is defined as our targeted intrinsic frequency.

B Spectral homogeneity of fMRI signals

The production of sub-figures (b)(c) in Figure 1 entails the computation of foregoing defined intrinsic frequencies of fMRI signals over harnessed HCP, ABIDE, and ACPI datasets. As shown in sub-figure (b)(c), the observed spectral homogeneity of fMRI signals is robust against the choice of parcellation atlases, and is ubiquitous in fMRI modality. One detrimental effect of the observed spectral homogeneity is its induced imprecise, coarse-grained spectral characterisation of whole-brain cortical activities, which cannot serve as a solid precursor for further spectral analysis.

C Datasets & Preprocessing

The resting-state fMRI HCP data from HCP900 release [4] served as our main investigation dataset on selected subjects ($N = 443$) with one scanning session (REST-1 of fMRI) and left-to-right phase encoding direction (1st run of one session). Each 3T scanned subject-wise data lasts for 14 mins

and 33s of each with 1200 volumes, 720 ms repetition time (TR), 33.1ms echo time (TE), and 2-mm isotropic voxel dimensions.

We adopted the suggested steps in released HCP dataset usage manual [2] to preprocess fMRI HCP data, including the correction from each T1-weighted image, the spatial alignment, and smoothing (kernel of 6-mm FWHM, and the Wishart filter), and regressed out the confounds (24 head-motion parameters).

We also include two independent validation datasets from the public available ABIDE and ACPI data bases. As the acquiring initiatives of two validation datasets were originated in neuropsychiatric studies, we then excluded all subjects that were confirmed to any current or history of mental illnesses. To minimise the multi-site scanning bias, only one site fMRI data were acquired from ABIDE and ACIP databases, forming two validation datasets: ABIDE-HC and ACPI-HC.

D Empirical comparison with alternative approaches

In attached Figure 6, we demonstrate the empirical performance of implementing our approach and three alternatives, e.g., the functional PCA, coroICA, and SOBI approaches, on transforming the original fMRI signals from HCP dataset. With respect to the assessed distributions of spectral characters, our temporal de-correlation approach leads to the most drastic improvement on the spectral resolution of signals among four transformation approaches, i.e., the transformed signals have widest frequency range, and a bimodal distribution of spectral characters.

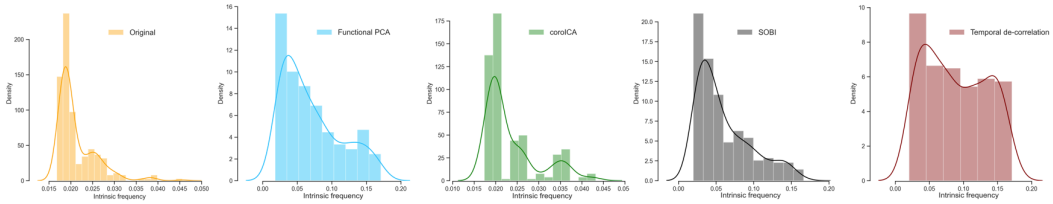

Figure 6: **Empirical comparison between our approach and alternatives.**

E Enlarged spectral dissimilarity of temporal de-correlated fMRI signals

Aside from the assessed spectral character, the improvement on spectral resolution of temporal de-correlated signals is also reflected as the observed enlargement on spectrum dissimilarity among signals. Since the quantified dynamic time warping (DTW) distance among spectrum is able to inform us the spectral dissimilarity among signals, as indicated in the following Figure 7, our transformed temporal de-correlated signals attain much larger spectral dissimilarity than the original ones.

[2] `https://www.humanconnectome.org/storage/app/media/documentation/s900/HCP_S900_Release_Reference_Manual.pdf`

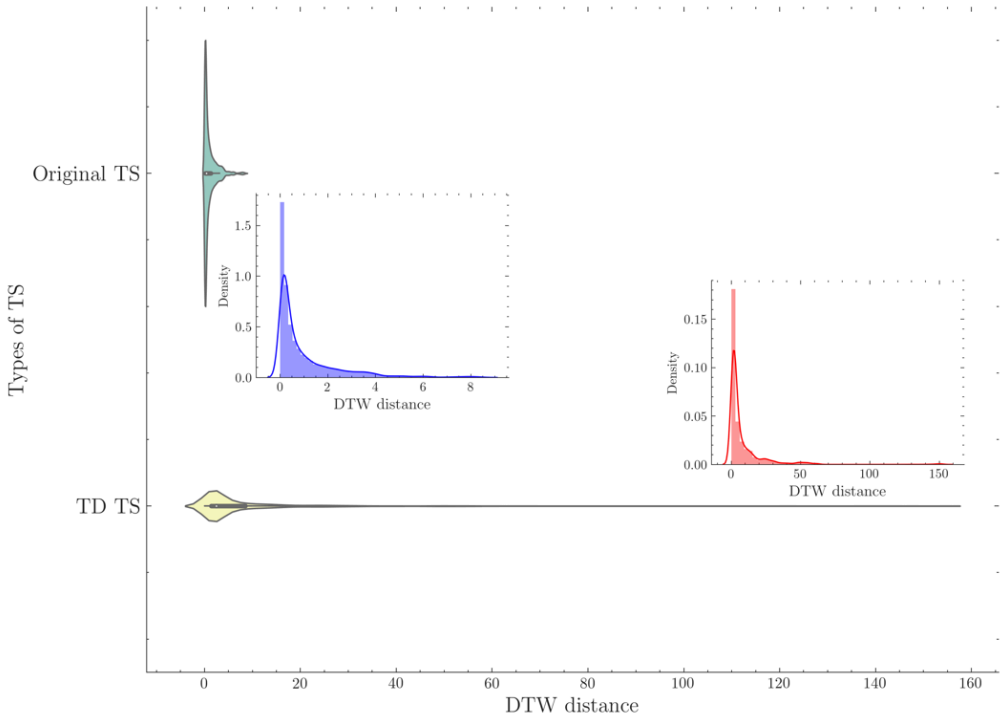

Figure 7: **Pair-wise DTW distance among estimated spectrum from the original and temporal de-correlated HCP fMRI signals.** Abbreviation index: TD TS: temporal de-correlated time series.